Design and Control of a Robotic Exoskeleton Glove Using a Neural Network Based Controller for Grasping Objects

Sarthak Pradhan

Thesis submitted to the Faculty of the
Virginia Polytechnic Institute and State University
in partial fulfillment of the requirements for the degree of

Master of Science
in
Mechanical Engineering

Pinhas Ben-Tzvi, Chair
Corina Sandu
Steve Southward

July 23, 2021
Blacksburg, Virginia

Keywords: Exoskeleton glove, Rotary SEA, Abduction Adduction Mechanism, Neural Network , Force Estimation.

Design and Control of a Robotic Exoskeleton Glove Using a Neural Network Based Controller for Grasping Objects

Sarthak Pradhan

(ABSTRACT)

Patients suffering from brachial plexus injury or other spinal cord related injuries often lose their hand functionality. They need a device which can help them to perform day to day activities by restoring some form of functionality to their hands. A popular solution to this problem are robotic exoskeletons, mechanical devices that help in actuating the fingers of the patients, enabling them to grasp objects and perform other daily life activities. This thesis presents the design of a novel exoskeleton glove which is controlled by a neural network-based controller. The novel design of the glove consists of rigid double four-bar linkage mechanisms actuated through series elastic actuators (SEAs) by DC motors. It also contains a novel rotary series elastic actuator (RSEA) which uses a torsion spring to measure torque, passive abduction and adduction mechanisms, and an adjustable base. To make the exoskeleton glove grasp objects, it also needs to have a robust controller which can compute forces that needs to be applied through each finger to successfully grasp an object. The neural network is inspired from the way human hands can grasp a wide variety of objects with ease. Fingertip forces were recorded from a normal human grasping objects at different orientations. This data was used to train the neural network with a R2 value of 0.81. Once the grasp is initiated by the user, the neural network takes inputs like orientation, weight, and size of the object to estimate the force required in each of the five digits to grasp an object. These forces are then applied by the motors through the SEA and linkage mechanisms to successfully grasp an object autonomously.

Design and Control of a Robotic Exoskeleton Glove Using a Neural Network Based Controller for Grasping Objects

Sarthak Pradhan

(GENERAL AUDIENCE ABSTRACT)

Humans are one of the few species to have an opposable thumb which allows them to not only perform tasks which require power, but also tasks which require precision. However, unfortunately, thousands of people in the United States suffer from hand disabilities which hinder them in performing basic tasks. The RML glove v3 is a robotic exoskeleton glove which can help these patients in performing day to day activities like grasping semi-autonomously. The glove is lightweight and comfortable to use. The RML glove v3 uses a neural network based controller to predict the grasp force required to successfully grasp objects. After the user provides the required input, the glove estimates the object size and uses other inputs like object orientation and weight to estimate the grasp force in each finger linkage mechanism. The motors then drive the linkages till the required force is achieved on the fingertips and the grasp is completed.

Acknowledgments

I would like to thank Professor Pinhas Ben-Tzvi for his constant guidance and support. I would also like to thank the ME department for funding me as a TA. I would like to thank Yunfei Guo and Wenda Xu for our collaboration to successfully design and manufacture the RML GLove V3. I would also like to thank all of my lab members for supporting me throughout.

Research reported in this publication was supported by the Eunice Kennedy Shriver National Institute of Child Health & Human Development of the National Institutes of Health under Award Number R21HD095027. The content is solely the responsibility of the authors and does not necessarily represent the official views of the National Institutes of Health.

Contents

List of Figures

List of Tables

List of Abbreviations

ADL: Activities of Daily Living

ANN: Artificial Neural Network

DOF: Degree of Freedom

FSR: Force Sensing Resistor

IMU: Inertial Measurement Unit

ReLU: Rectified Linear Unit

RML glove v3: Version 3 of Exoskeleton designed in Robotics and Mechatronics Lab

RSEA: Rotary Serial Elastic Actuator

SEA: Serial Elastic Actuator

Chapter 1

Introduction

1.1 Background

Human hands are very complex and can perform a variety of grasps, like cylindrical, palmar, hook, lateral, tip, spherical, etc. [1]. Unfortunately, there are approximately 296,000 [13] people suffering from spinal cord injury and 795,000 [14] stroke patients in the United States. These patients often have reduced hand capabilities and face problems in performing the activities of daily life (ADLs). Hence, there is a huge demand for robotic exoskeletons which are basically mechanical devices consisting of linkages, tendons or cables, and different types of actuation systems. The glove, in our case, focuses on patients suffering from brachial plexus injury where the patient has a reduced hand capability from below the shoulder. The patient has functional elbow and shoulder but the human hand is very complex and its very difficult to restore hand functionality. Thus, the RML Glove V3 aims at actuating only the fingers and wrist to help the users in performing basic grasping activities semi-autonomously. The glove along with an efficient design also needs a robust control algorithm to enable it to grasp objects with ease. According to the best of authors' knowledge, not much research has been done on controls involving exoskeleton gloves.

Figure 1.1: Different types of grasps performed by humans [1]

1.2 Contributions

In this thesis, a novel exoskeleton glove was designed with a new rotary series elastic actuator (RSEA), a passive adduction/abduction mechanism, and an adjustable base. A neural network based control algorithm was also designed to determine the force output among the fingertips to successfully grasp an object. This algorithm was then tested on the glove prototype, the RML Glove V3.

1.3 Thesis Structure

A brief overview of each chapter is listed as follows:

Chapter 1: Gives a brief introduction about the exoskeleton glove and outlines the reasons why people use them.

Chapter 2: Discusses state of the art exoskeleton gloves in terms of their design and the control algorithms used to control them.

Chapter 3: Discusses the problem statement and the proposed solution.

Chapter 4: Provides details regarding the hardware design of our RML Glove V3 and discusses various components of this glove in depth.

Chapter 5: Presents the fingertip force data collection process required for the neural network and also discusses the hyper-tuning process to determine the neural network architecture used.

Chapter 6: Provides the size estimation process required to determine one of the inputs and presents the experimental results of the controller used with the RML Glove V3 to grasp objects.

Chapter 7: Concludes the thesis and discusses the future work that can be done to improve the control algorithm and the RML Glove V3.

1.4 Selected Publications

Disclosure: Contents from these publications are used in this thesis.

1.4.1 Peer-Reviewed Journal Paper

1: Pradhan, S., Guo, Y., Xu, W., Bravo, C.J., Ben-Tzvi, P., "Control of an Exoskeleton Glove for Grasping Objects using Neural Networks" Journal of Mechanism and Robotics, submitted, August 2021.

2: Guo, Y., Xu, W., Pradhan, S., Bravo, C.J., Ben-Tzvi, P., "Data Driven Calibration and Control for Compact Lightweight Series Elastic Actuators for Robotic Exoskeleton Gloves", IEEE Sensors Journal, Published online, July 2021. DOI: 10.1109/JSEN.2021.3101143

3: Guo, Y., Xu, W., Pradhan, S., Bravo, C.J., Ben-Tzvi, P., "Personalized Voice Activated Grasping System for a Robotic Exoskeleton Glove", Mechatronics Journal, accepted with revisions, July 2021.

1.4.2 Peer-Reviewed Conference Paper

1: Pradhan, S., Xu, W., Guo, Y., Bravo, C.J., Ben-Tzvi, P., "A Novel Design of a Robotic Glove System for Patients with Brachial Plexus Injuries", Proceedings of the 2020 ASME IDETC/CIE, 44th Mechanisms & Robotics Conference, St. Louis, MO, Aug. 16-19, 2020.

2: Xu, W., Pradhan, S., Guo, Y., Bravo, C.J., Ben-Tzvi, P., "Integrated and Configurable Voice Activation and Speaker Verification System for a Robotic Exoskeleton Glove", Proceedings of the 2020 ASME IDETC/CIE, 44th Mechanisms & Robotics Conference, St. Louis, MO, Aug. 16-19, 2020.

Chapter 2

Literature Review

Exoskeleton gloves are devices designed to assist users by either increasing their grasp force or by guiding their fingers towards the appropriate trajectories in order to perform various tasks like grasping. There have been various types of exoskeleton gloves developed in the past, either for aiding patients suffering from hand disabilities, or for providing users with a sense of touch in virtual reality. One class of exoskeleton gloves consists of rigid mechanical structures and linkages. These mechanisms have a good force transmission and repeat-ability, but may be extremely bulky and uncomfortable to use. The other class of exoskeleton gloves consists of tendons or other compliant mechanisms and are referred to as soft exoskeleton gloves. These types of exoskeleton gloves are generally compact and lightweight. The main drawbacks of these types of glove mechanisms are frictional losses during force transmission, low durability, and bad repeat-ability.

2.1 Hardware Design

2.1.1 RML Glove

There have been several versions of exoskeleton gloves developed in our Robotics and Mechatronics Lab [4, 15, 16]. The latest glove developed till the RML Glove V3 is the RML Glove [2] which is a rigid exoskeleton glove consisting of rigid mechanical linkages connected to

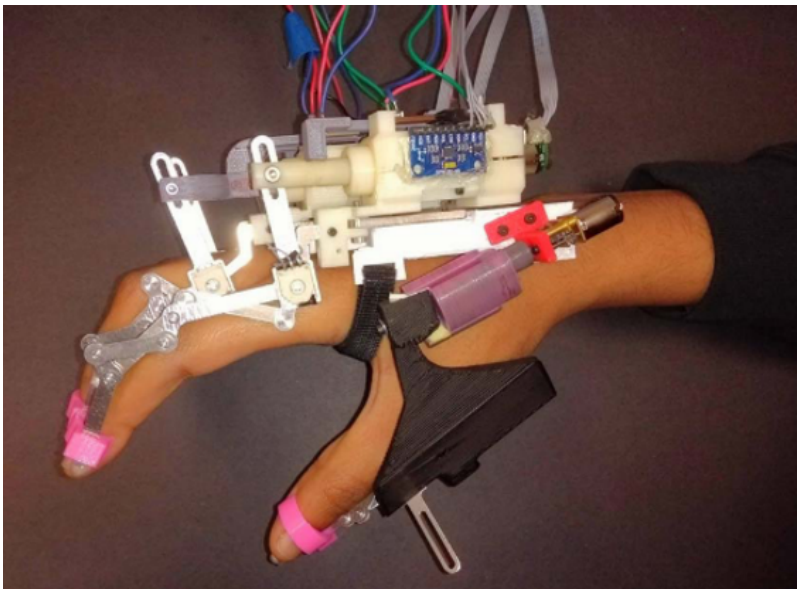

Figure 2.1: RML glove with SEAs and linkages attached to a human hand [2]

series elastic actuators (SEAs). The linkages allow for natural bending profiles and the glove can measure forces at the fingertips through the SEAs. However, the glove does not allow the natural ab/adduction of human fingers as all of the SEAs are rigidly attached to the base. This version of the glove also does not have a way to measure the torque applied through the thumb as a rotary series elastic actuator has not been implemented.

2.1.2 Hand Exoskeleton Glove with Parallelogram Mechanism

This hand exoskeleton glove consists of rigid linkages actuated by motors designed to apply forces on the tips of the index finger and the thumb [3]. The design only consists of the index finger and thumb mechanisms which allows for both ab/adduction and flexion/extension. In this glove, the rotation between the distal and middle phalanx has been coupled with the rotation between the middle and the proximal phalanx with the help of a crossed parallelogram mechanism. The design uses a three-motors-in-one-finger mechanism which weighs 0.51kg. The overall exoskeleton weighs 1.1kg. This exoskeleton can apply forces ranging from 0-5 N,

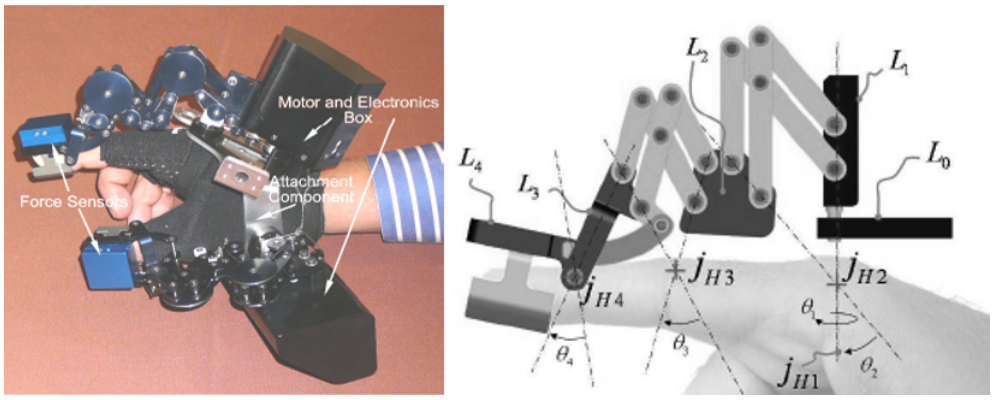

Figure 2.2: Hand Exoskeleton glove consisting of a parallelogram mechanism actuated by the motor and electronics box [3]

which is quite low and will cause difficulty in grasping heavy objects. Another disadvantage of this exoskeleton glove is its bulky size and weight which can cause discomfort to the user.

2.1.3 iSAFER

The iSAFER [4] is the successor of the SAFER [17] glove and consists of rigid mechanical linkages actuated through cables and pulleys. Each of the bidirectional cables are actuated through a single motor due to which each finger mechanism requires only one motor while the thumb requires two motors. This exoskeleton glove also consists of a pivot in the base of each linkage mechanism which allows for passive adduction and abduction. On top of that, this glove also consists of a rotary potentiometer and two force sensors located at each fingertip to allow for angular position measurement and force measurement respectively. This glove is also able to fit users with varying hand widths and thicknesses. The iSAFER glove is able to detect slippage and increase the force output to grasp the object stably. Although the glove is lightweight, the rigid links attached on top of each finger make the overall design bulky.

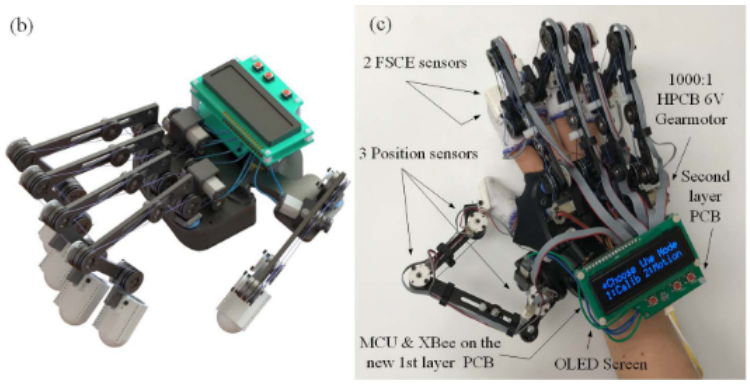

Figure 2.3: iSAFER glove with tendon driven rigid linkage mechanism [4]

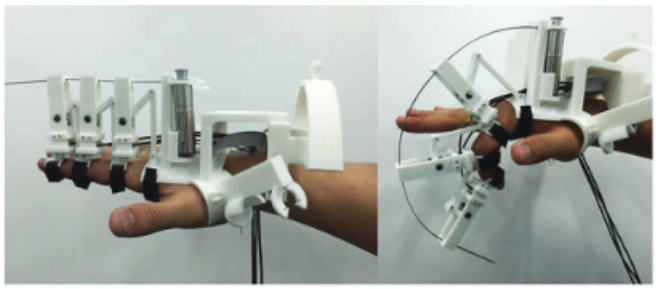

Figure 2.4: Hand Exoskeleton with carbon composite strip connected to mechanical links [5]

2.1.4 Hand Exoskeleton with Carbon Strip

This cable-driven hand exoskeleton [5] as shown in Fig. 2.4 was designed for the bio-mechanical analysis of the stroke hand. The design consists of rigid links guided by a carbon composite strip which allows for the fingers to bend. This glove contains five actuators, one on each finger, which drive these flexible strips and provide the required force. The drawback of this type of design is that the cables and links attached on top of each finger make the exoskeleton glove system large and bulky which can make it uncomfortable for the user to use it.

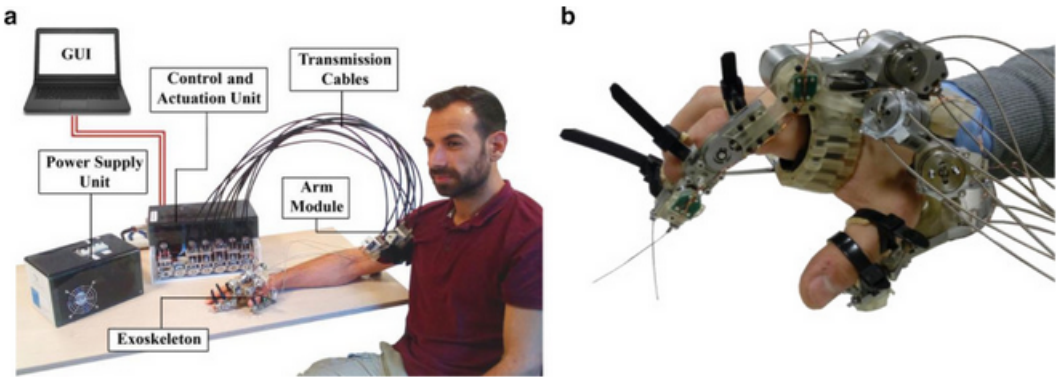

Figure 2.5: HandeXos-Beta with bench-top control and actuation unit [6]

Figure 2.6: Portable Exoskeleton Glove With Soft Structure [7]

2.1.5 HandeXos-Beta

The HandeXos-Beta glove [6] only consists of the index finger and thumb mechanisms capable of producing fingertip output forces of around 4 N. The two-staged Bowden cables are coupled with the actuators which allow for the flexion and extension of the digits. This device also contains series elastic actuators (SEA) which make it capable of measuring applied torque with ease. 14 sensors are attached to this system for torque and position measurement. It also contains passive degrees of freedom in the index and thumb mechanisms which allows for better adjust-ability. The exoskeleton weighs around 420g. The overall system also requires a bench-top control and actuation unit, and a battery unit, which can make it not very portable.

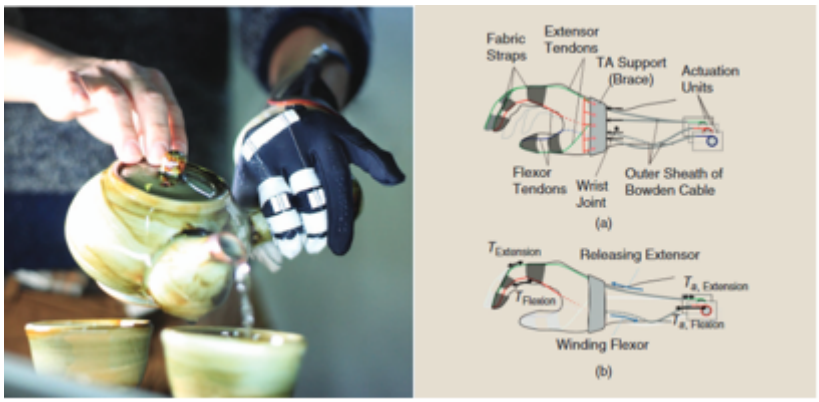

Figure 2.7: Exo-Glove [8]

2.1.6 Portable Exoskeleton Glove with Soft Structure

This soft exoskeleton glove [7] basically consists of an inner soft glove, a second layer of stiff material to support the actuators and cables, actuators, and an optional layer to cover up the cables and actuators. The design has the ability to actuate the thumb and the first three fingers. Each finger is attached with a pair of cables passing through guides on both the frontal and dorsal part of the finger which control its flexion and extension. The total weight of this glove system is 340g. The overall system is lightweight and only consists of 4 DC motors as actuators. This glove design is missing an abduction/adduction degree of freedom which can cause problems while grasping. Another drawback can be the soft structure of the glove which can make it bend or twist undesirably while applying force to perform the grasping.

2.1.7 Exo-Glove

The Exo-Glove [8] is a soft exoskeleton glove which has a tendon routing system. This design has tendons attached to the index finger, middle finger, and thumb which are actuated by motors inside an actuation unit. The design has PTFE tubes which act as pulleys for the

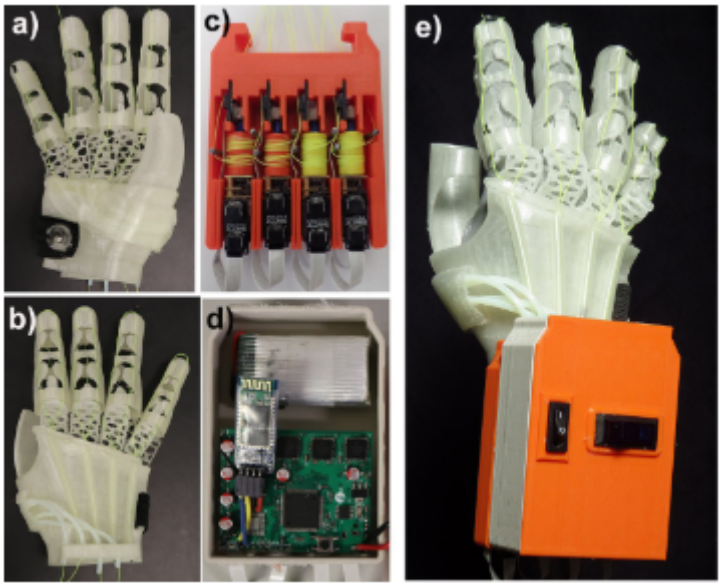

Figure 2.8: Flexo-Glove [9]

tendons and minimizes the stretching of the gloves by the tendons while performing the flexions and extensions. Pretension is avoided in this glove which makes it more comfortable for the users. The glove has a simplistic and compact design which weighs around 194g. The overall system is lightweight and compact, but it only accounts for three fingers for grasping. Also, the tendon mechanisms can suffer from frictional losses and repeat-ability issues.

2.1.8 Flexo-Glove

The proposed design of the Flexo-Glove [9] consists of a soft, 3D-printed structure which has cables attached to each of the four fingers. The thumb does not have any actuation, but is held rigidly in a certain position. The cables are pulled by a motor with the help of a spool which actuates the fingers. The glove is compact and the weight of the glove is 330g which makes it relatively lightweight and also capable of applying 22N pinch force. However, one of the main drawbacks of this type of design is the lack of mobility of the thumb. Also, as with cable mechanisms in soft structures, it is susceptible to frictional losses, repeat-ability

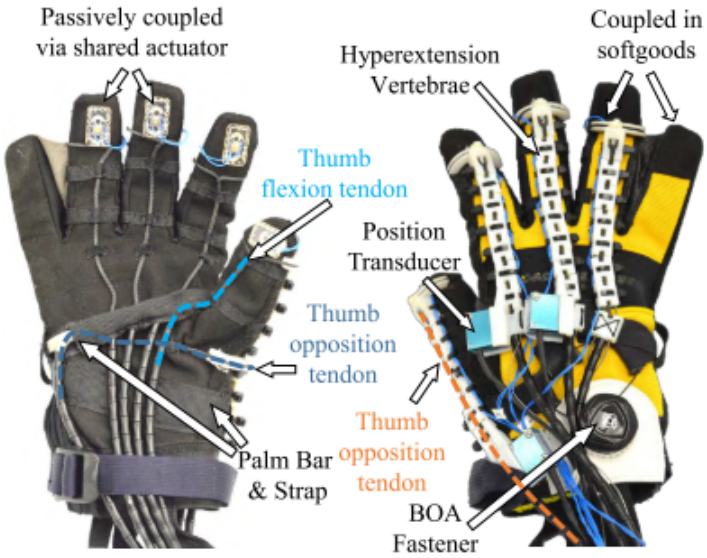

Figure 2.9: SPAR glove [10]

issues, and undesired deformations.

Over the recent years, a lot of hybrid mechanisms have also been developed which incorporate different features from soft and rigid exoskeleton gloves in an attempt to improve its grasping capability and overall performance.

2.1.9 SPAR Glove

The SeptaPose Assistive and Rehabilitative (SPAR) Glove [10] is a hybrid glove consisting of both rigid and soft elements. It has a segmented vertebrae-like structure in the back of the fingers of a soft glove to provide for rigidity and prevents hyper-extension. The fingers are actuated through a Bowden cable transmission mechanism. The little finger and the ring finger are coupled while the middle finger and the ring finger share an actuator which reduces the number of motors required. However, the total weight of the glove system is 16kg which can cause portability issues. Another drawback can be the weak joints between the rigid and soft elements of the glove.

Figure 2.10: Hybrid Exoskeleton Glove with a Telescopic Thumb [11]

2.1.10 Hybrid Exoskeleton Glove with a Telescopic Thumb

This hybrid glove [11] consists of internal cables and motors to flex or extend all of the fingers, but the ring finger and the little finger are coupled to a single motor. It also has soft jamming structures comprised of jamming layers that are attached on top of all five digits which work with the help of a vacuum pump connected through tubes. When a vacuum is applied, it makes the soft jamming structures stiff which helps with grasping. The abduction and adduction of the fingers is also pneumatically actuated. There is also an extra soft structure attached to the bottom of the palm of the glove to help with grasping.

2.2 Control Algorithms

2.2.1 Control of RML Glove Using an Iterative Approach

The previous version of the RML glove developed by Teja et.al [2] used an iterative based method to find the optimal forces that must be applied by each finger linkage mechanism

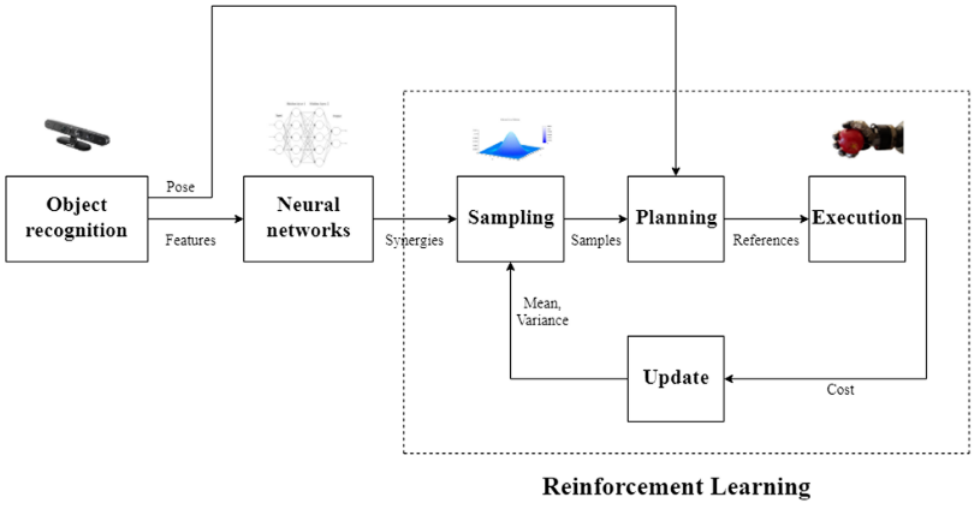

Figure 2.11: Proposed Algorithm [12]

to successfully grasp an object. This type of control algorithm uses a random set of initial values of force for each of the five fingers and then tries to find the optimal solution using the interior point method in an iterative manner. It uses the equations of force and torque balance as constraints along with some inequality constraints given by motor specifications. The iterative approach to generate solutions can be computationally expensive and time-consuming.

2.2.2 Vision Based Grasp using Neural Network and Reinforcement Learning

The algorithm proposed in this research [12] uses a combination of computer vision, neural networks and reinforcement learning to enable a robotic system to grasp objects. Computer vision is used to recognize objects and extract features from them which are then used as inputs by the neural network which has been trained using human demonstrations. These neural network parameters in-turn were then used to initialize reinforcement learning which helps the robotic system to keep improving.

Chapter 3

Problem Statement and Proposed Solution

The aim of the exoskeleton glove is to help users that struggle to grasp objects autonomously at different orientations. To achieve this goal, the exoskeleton needs to both have an appropriate mechanical design, and an appropriate control algorithm. When it comes to the design aspect, the glove needs to be light-weight, portable, comfortable, able to follow natural bending paths, and have the capacity to apply and measure force. Secondly, to grasp the object successfully, the finger mechanisms need to apply the appropriate amount of force based on the angular position, size, and weight of the object.

The previous versions of the RML gloves were bulkier and did not allow for natural abduction and adduction of the fingers while grasping. To accommodate users of different hand sizes, the current glove consists of an adjustable base and an abduction mechanism. The glove also consists of a novel rotary series elastic actuator mechanism which is very efficient and relatively smaller in size. Also, in this research, a neural network based control algorithm is used to determine the force distribution among all five digits in order to successfully grasp an object.

Chapter 4

Hardware Design of Robotic Exoskeleton Glove

4.1 Design Overview

The RML Glove V3 [18] is a rigid exoskeleton glove designed and manufactured in the Robotics and Mechatronics Lab at Virginia Tech by a team consisting of Sarthak Pradhan, Yunfei Guo, and Wenda Xu as shown in Fig. 4.1. This glove was designed for patients suffering from brachial plexus injury who need help with actuating their fingers and wrists. Unlike most rigid exoskeleton gloves, our exoskeleton glove consists of thin linkage mechanisms which are attached beside the finger. Each of the five linkage mechanisms are attached to series elastic actuators (SEA) which enable force measurement and compliance. The thumb mechanism also consists of a rotary series elastic actuator (RSEA) which is then attached to the thumb base containing the thumb SEA and linkage mechanism. Overall, the RML Glove V3 consists of 5 linear SEAs, 1 rotary SEA, 5 (1 DOF) linkage mechanisms, a micro-controller (Teensy 4.1), a battery, and other electronics. The battery can support our glove for about 2 hours of operation.

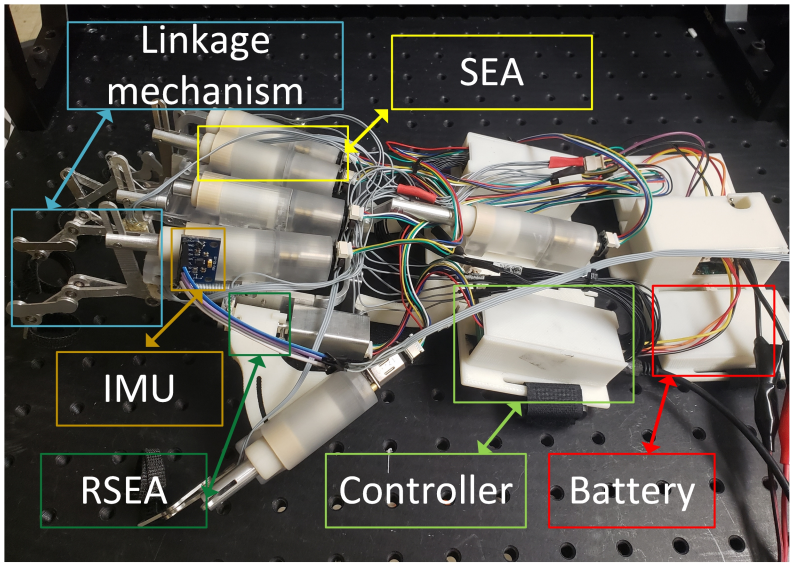

Figure 4.1: Manufactured version of the RML Glove V3 with SEAs, linkage mechanisms, IMU and electronics

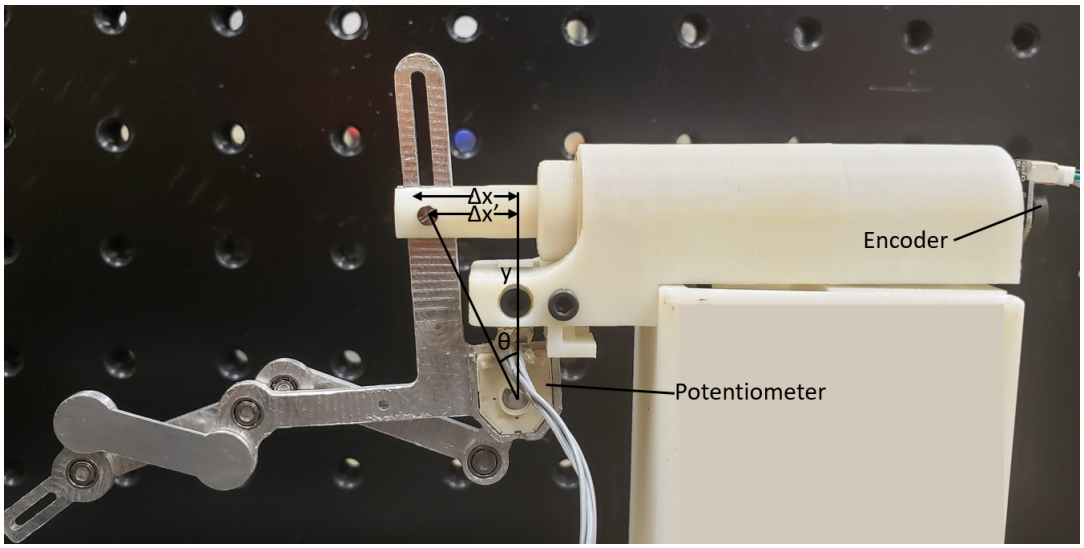

Figure 4.2: Prototype of index SEA along with the its linkage mechanism

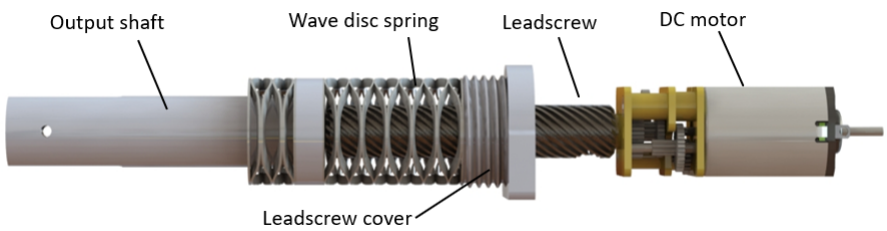

Figure 4.3: Inner view of the linear SEA

4.1.1 Linear Series Elastic Actuator

The linear series elastic actuator is a device which transmits and measures force from the motor to the output shaft. The design of the current linear SEA is based on Refour et al [15]. It consists of an inner mechanical part (lead-screw cover) attached to the motor, a wave disc spring, and an outer mechanical part (output shaft) in mechanical contact with the spring as shown in Fig. 4.3. The force applied by the SEA can be measured by multiplying the spring constant with the difference in displacement measured by the motor encoder and potentiometer attached to the base of the linkage mechanism. This force can be calculated through the equations 4.1 and 4.2.

$$F_{out} = K_{linear} \cdot (\Delta x - \Delta x') \tag{4.1}$$

$$\Delta x' = y \cdot (tan(\theta)) \tag{4.2}$$

where,

K_{linear} – is the linear spring constant.

$\Delta x'$ – is the displacement of the output shaft measured by the potentiometer attached to linkage base.

Δx – is the actual displacement of the output shaft measured by the motor encoder.

y – is the perpendicular distance from the joint to the output shaft.

θ – is the angle made by the base of the linkage mechanism with the vertical axis.

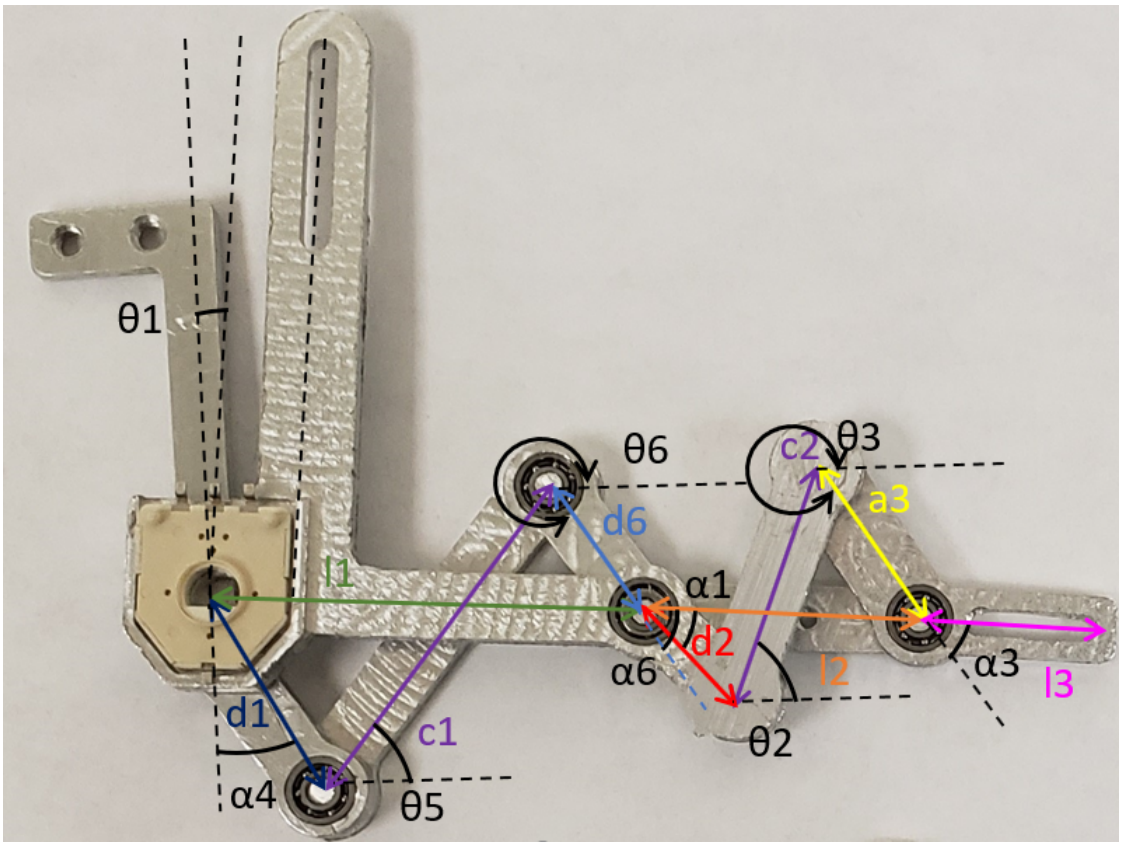

Figure 4.4: Linkage mechanism with labels for different dimensions of the links

4.1.2 Linkage Mechanism

The design of the mechanical linkages that is responsible for transmitting forces from motors to fingers is based on a previous version of the RML glove [19]. However the pin joints of the previous mechanism were replaced with bearing joints to minimize backlash and friction as shown in Fig. 4.4. It also contains a potentiometer to measure the angle subtended by the first link with the fixed link of the mechanism. Each of these mechanical linkages has a single degree of freedom and consists of a double four-bar mechanism where the link lengths are optimized in a way to follow natural finger bending profiles. The kinematics of this linkage mechanism can be solved with the help of equations 4.3-4.6 and simulated in a programming environment as shown in Fig. 4.5.

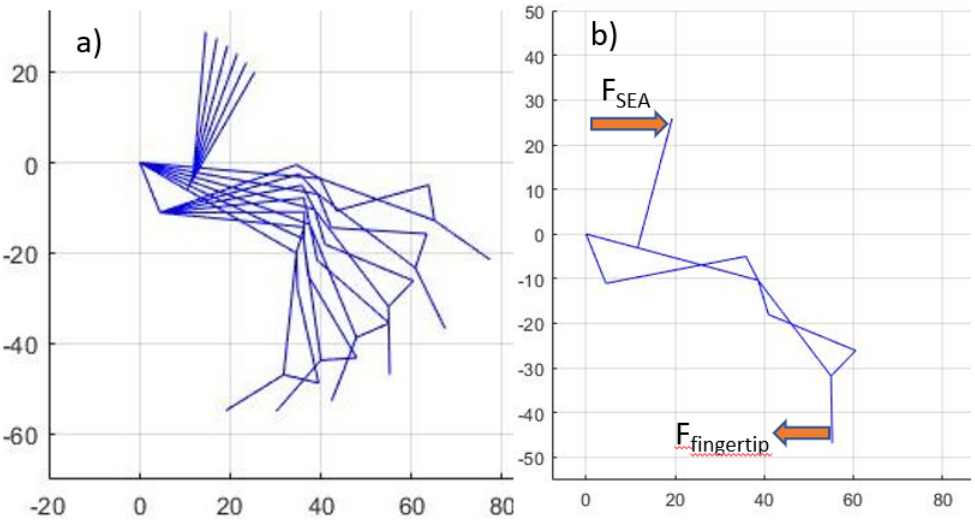

Figure 4.5: a) Matlab simulation of the linkage mechanism, b) Linkage mechanism acting as a lever to transfer force from SEA to the fingertip

$$d_1 \cdot sin(\alpha_4) + c_1 \cdot cos(\theta_5) + d_6 \cdot cos(\theta_6) - l_1 \cdot cos(\theta_1) = 0 \tag{4.3}$$

$$-d_1 \cdot cos(\alpha_4) + c_1 \cdot sin(\theta_5) + d_6 \cdot sin(\theta_6) - l_1 \cdot sin(-\theta_1) = 0 \tag{4.4}$$

$$d_2 \cdot cos(\theta_1 + \alpha_1) + c_2 \cdot cos(\theta_2) + a_3 \cdot cos(\theta_3) - l_2 \cdot cos(\theta_6 + \alpha_6) = 0 \tag{4.5}$$

$$-d_2 \cdot sin(\theta_1 + \alpha_1) + c_2 \cdot sin(\theta_2) + a_3 \cdot sin(\theta_3) - l_2 \cdot sin(\theta_6 + \alpha_6) = 0 \tag{4.6}$$

where,

$\theta_1, \theta_2, \theta_3, \theta_5, \theta_6$ – angle subtended by the links with x-axis.

l_1, l_2, l_3 – lengths of links corresponding to proximal,

middle, distal phalanxes.

c_1, c_2 – constraint lengths.

d_1, d_2, d_6, a_3 – length parameters of links.

$\alpha_1, \alpha_3, \alpha_4, \alpha_6$ – angular parameters of the links.

The force produced by the motor is transmitted by the SEA through the output shaft which is mechanically connected to the first link of the linkage mechanism. The output force at the fingertip is then transmitted though the entire linkage mechanism which varies according to the base angle of the linkage. The mechanical leverage of the linkage mechanism, which is the ratio of the output force to the input force, can be calculated by equation 4.7.

$$Lev = \frac{sea_{height}}{|(\vec{r}_{fingertip} \times \vec{F}_{ang})|} \tag{4.7}$$

The distance vector and the force vector required to calculate the torque can be calculated using equations 4.8 and 4.9 respectively.

$$r_{fingertip} = [x_{fingertip}, y_{fingertip}, 0] \tag{4.8}$$

$$F_{ang} = [cos(\theta_3 + \alpha_3 + pi/2), sin(\theta_3 + \alpha_3 + pi/2), 0] \tag{4.9}$$

The x and y components of the distance vector can be calculated from the equations 4.10 and 4.11 respectively.

$$\begin{aligned} x_{fingertip} = (l_1 \cdot cos(-\theta_1) + d_2 \cdot cos(\theta_1 + \alpha_1) \\ +c_2 \cdot cos(\theta_2)) + a_3 \cdot cos(\theta_3) + l_3 \cdot cos(\theta_3 + \alpha_3)) \end{aligned} \tag{4.10}$$

$$\begin{aligned} y_{fingertip} = (l_1 \cdot sin(-\theta_1) + d_2 \cdot sin(\theta_1 + \alpha_1) \\ +c_2 \cdot sin(\theta_2) + a_3 \cdot sin(\theta_3) + l_3 \cdot sin(\theta_3 + \alpha_3)) \end{aligned} \tag{4.11}$$

where,

Lev – leverage of the linkage mechanism.

sea_{height} – vertical distance of the output shaft from the base joint of the linkage mechanism.

T – torque applied through the linkage mechanism

$r_{fingertip}$ – distance vector from the base joint to the fingertip

F_{ang} – angle of the force applied on the fingertip by the object being grasped

$x_{fingertip}$ – x-component of the $r_{fingertip}$ vector

$y_{fingertip}$ – y-component of the $r_{fingertip}$ vector

4.2 Design improvements from previous RML gloves

4.2.1 Rotary SEA

The new and improved rotary series elastic actuator (RSEA) consists of a tiny torsion spring sandwiched between the inner housing of the RSEA and the outer cover of the RSEA. The working principle of the RSEA is the same as a normal SEA. It uses a torsion spring as the compliant material to transmit torque through appropriate deflection. Firstly, the grasp is initiated and the motor rotates, which in turn rotates the entire thumb assembly which includes both the inner and outer RSEA. When the thumb comes in contact with the object while grasping, the outer part of the RSEA stops while the inner RSEA keeps rotating till a required torque is achieved. The torque applied can be calculated from the twist of the

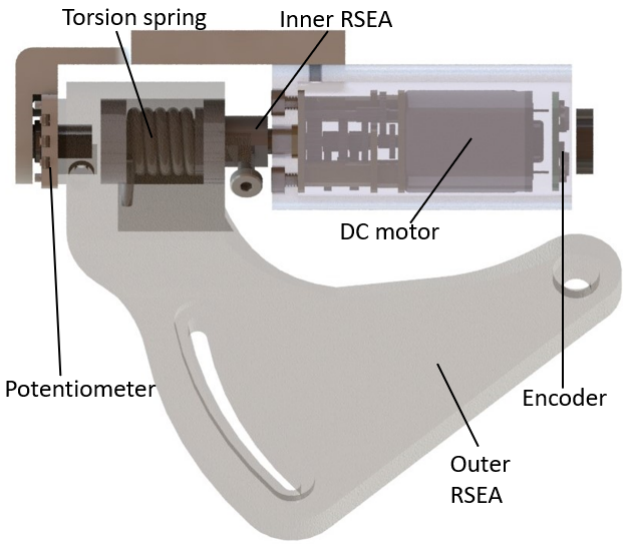

Figure 4.6: Inner view of the Rotary SEA. This shows the different components that make up the rotary series elastic actuator in a CAD model

torsion spring which can be measured by subtracting the values of the potentiometer attached in the front of and the encoder attached in the back of the RSEA. Since the torsion spring was modified to fit the mechanical design of the RSEA, the spring constant provided by the manufacturer cannot be used. Therefore, an experiment was conducted to both determine the spring constant (G), and to verify the working principle of the RSEA. A force sensor was placed in the appropriate location to record the fingertip force data corresponding to the deflection angle of the torsion spring. Deflections of 30, 40, 50, 60, 70, and 80 degrees were applied and the corresponding steady state force values were recorded which were converted to torque (T) by multiplying the moment arm from the rotation axis to the fingertip location. The data was plotted in Fig. 4.7 and a linear fit was used to obtain the line of equation 4.13 and the R^2 value of 0.9117 for that fit.

$$T = G \cdot \Delta\theta \tag{4.12}$$

$$T = 2.8215 \cdot \theta - 60.608 \tag{4.13}$$

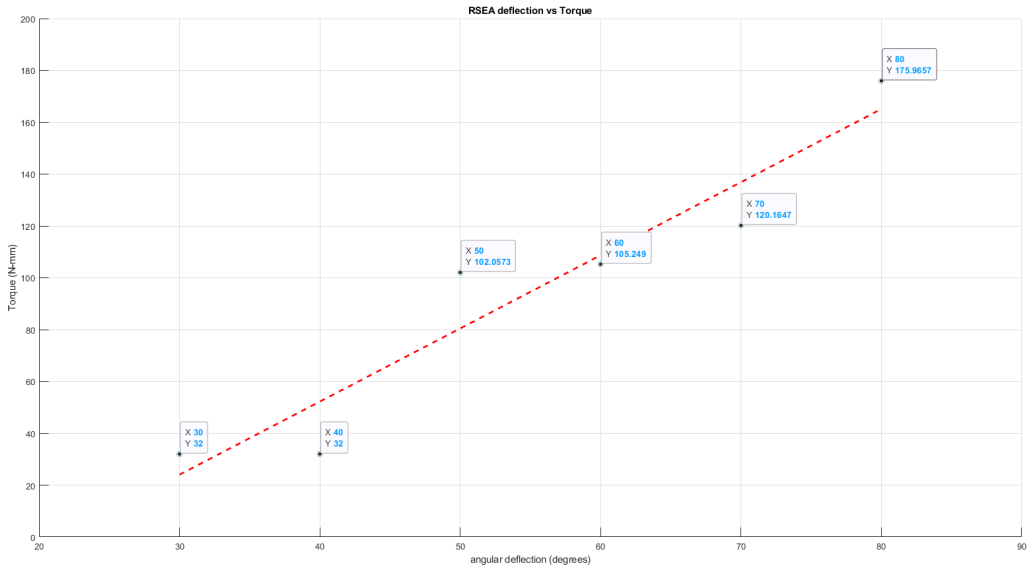

Figure 4.7: Deflection of torsion spring(degrees) in x-axis vs Torque(N-mm) in y-axis

where,

T – is the torque applied by the thumb motor in N-mm

G – is the torsion spring constant in N-mm/degrees.

θ_{r1} – is the angle measured in the back of the RSEA by the encoder attached to the motor in degrees.

θ_{r2} – is the angle measured in front of the RSEA by the potentiometer connected to the thumb base in degrees.

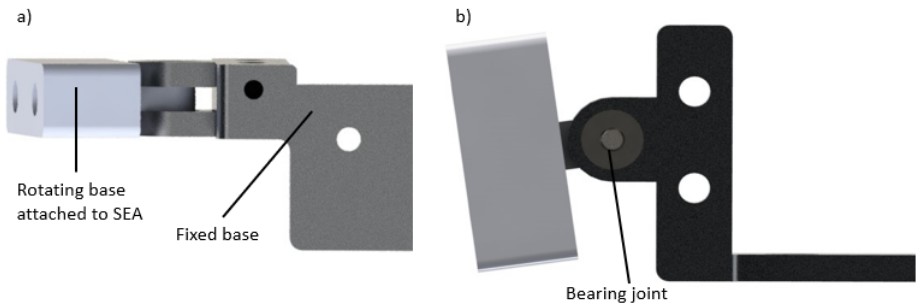

Figure 4.8: CAD design of the passive abduction/adduction mechanism consisting of a fixed base and a rotating base connected through a bearing joint

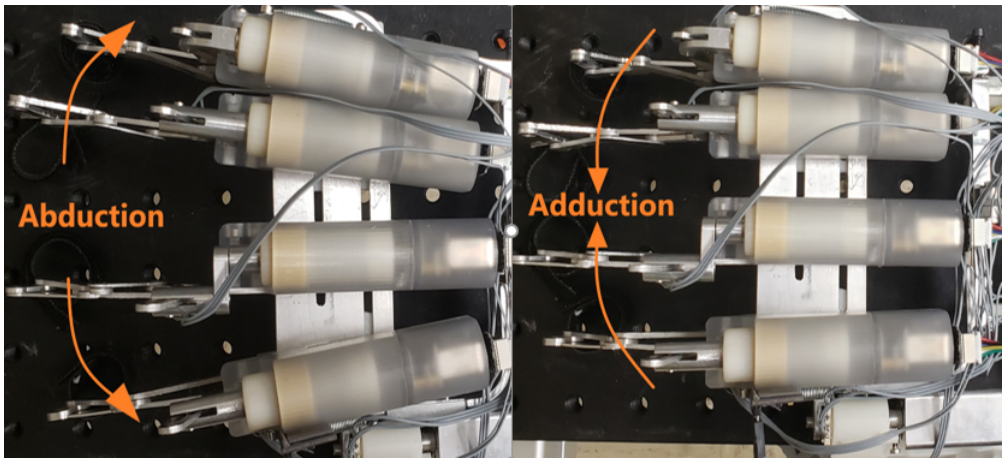

Figure 4.9: Passive abduction and adduction mechanism of the exoskeleton glove which provides more comfort and adjust-ability to users

4.2.2 Passive Abduction and Adduction Mechanism

Natural human fingers have the capability of abduction and adduction. Motors can be used to actuate the fingers to abduct and adduct, but this will make the glove too bulky and require more power to operate. To avoid this issue, a passive abduction and adduction mechanism was designed as shown in Fig. 4.8. It consists of the SEA attached on a base which rotates about the fixed base with the help of a bearing joint. The bases are kept in position with the help of a linear spring as shown in Fig. 4.9.

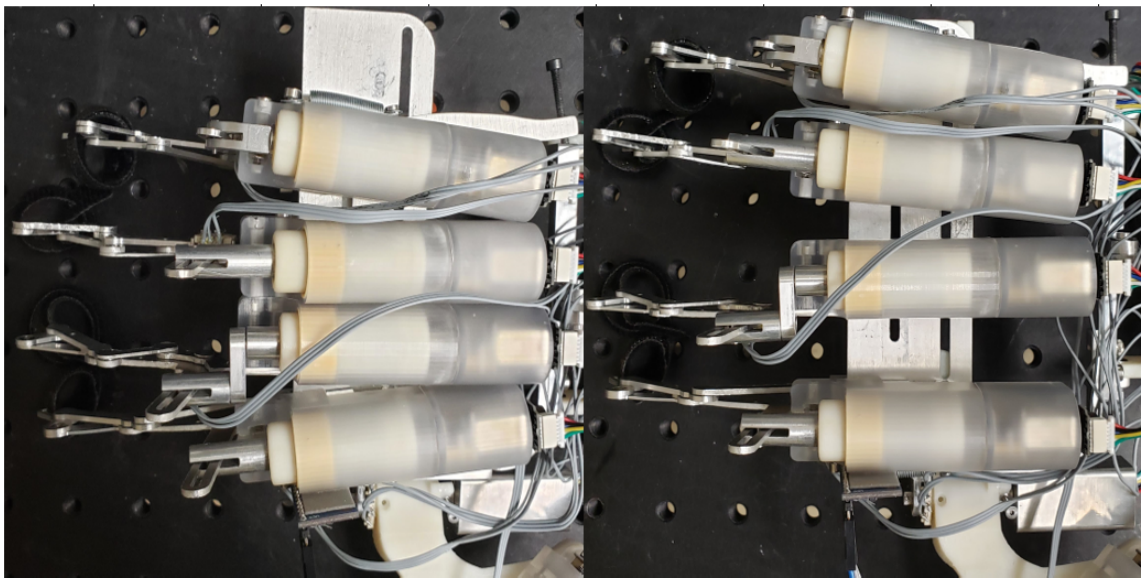

Figure 4.10: Adjustable base of the exoskeleton glove which allows for the finger mechanisms to slide and adjust to different hand sizes

4.2.3 Adjustable Base

Different users have different hand widths and thicknesses so one glove will not fit every user. The glove needs to be flexible enough to fit users of different hand sizes. This is why the new exoskeleton glove has an adjustable base consisting of slots which allow for the middle, ring, and little finger mechanisms to slide sideways, therefore accommodating different users as shown in Fig. 4.10. Owing to its adjust-ability, the RML Glove V3 can fit users with hand widths ranging from 90 mm to 110 mm.

Chapter 5

Neural Network Controller Design

5.1 Controller Design Principle

Humans frequently perform a wide variety of grasps effortlessly in their day to day lives. The idea behind the control algorithm is to learn the force pattern applied through the fingertips by an average human while grasping objects. Neural networks have been used in the past to learn different tasks by finding complex nonlinear mapping from the input to output data. Neural networks consist of an inner layer, a hidden layer, and an output layer comprised of neurons which are connected to each other through weights. In supervised, the training data is fed through the network repeatedly and the desired output data set is provided to it. The network adjusts its weights repeatedly through the process of back propagation until the desired accuracy is reached. The same concept is used in training the network after sufficient data has been collected from a normal human grasping objects of varying shapes and sizes at different orientations.

5.2 Experimental Setup and Data Collection

According to the best knowledge of the author, a complete data-set of force output at each finger while grasping objects at various orientations could not be found. Hence, an experimental setup was designed to record the force output at each fingertip while grasping

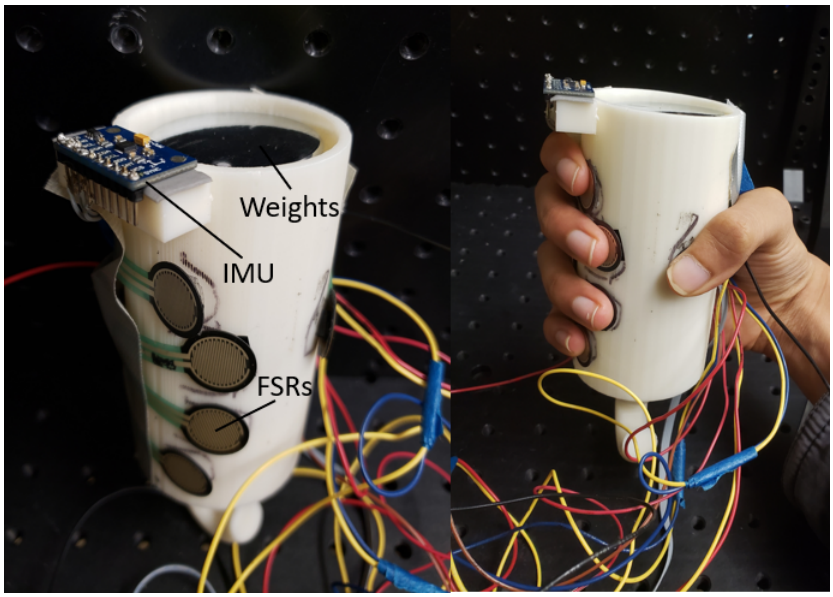

Figure 5.1: Test setup consisting of hollow cylindrical object attached with FSRs and IMU

cylinders of different radii and weights at different orientations. Three test subjects of different hand sizes were used to perform a cylindrical grasp. The setup consists of a hollow cylindrical object attached with force sensing resistors (FSRs) at fingertip positions and an inertial measurement unit (IMU) on top. The weight of this cylinder can be gradually increased by adding weights inside of it. The test subjects grasped the cylinders of different diameters ranging from 46mm to 86mm at different orientations while the force data of all five digits, angular position, weight, and size of the cylinder were recorded.

5.3 Hyper-parameter Tuning

As shown in Fig. 5.2, the neural network consists of an input layer with 4 neurons representing the size, weight, and orientation of the object, a hidden layer, and an output layer with 5 neurons representing the 5 forces required at the users fingertips. The structure of the hidden layer and the activation function to be used also need to be determined for this

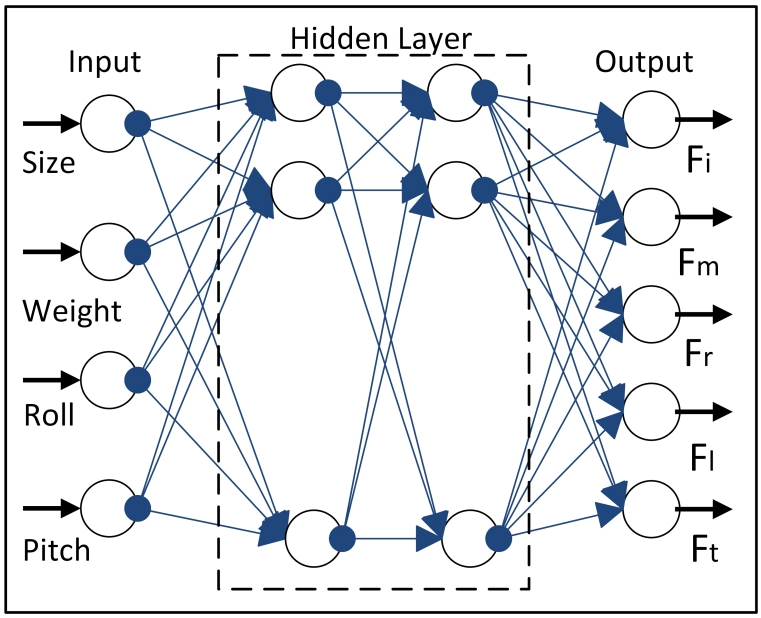

Figure 5.2: Neural network model with an input layer, 2 hidden layers, and an output layer with 5 neurons representing fingertip forces

network. Hyper parameter tuning is a process to determine an optimal neural network architecture which will obtain a low mean squared error and a high correlation between the inputs and the outputs. The neural network architecture in this case refers to the number of neurons in each hidden layer. The GridSearchCV search was used from the scikit-learn library to search a set of values of neurons in hidden layers which gives a high R^2 value. The results are shown in Table. 5.1.

Table 5.1: R^2 value of neural network using different number of neurons and activation function

hidden layer sizes	activation	mean R^2
(300, 400)	relu	0.70270968
(400, 300)	relu	0.7027547
(300, 400)	logistic	0.49535212
(400, 300)	logistic	0.50721706
(300, 400)	tanh	0.6225991
(400, 300)	tanh	0.64120692

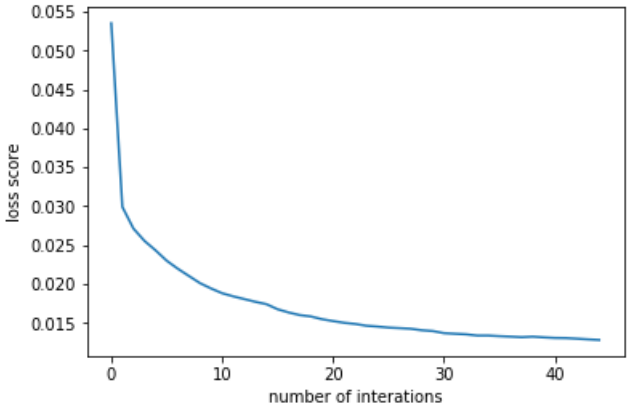

Figure 5.3: Loss score while training vs. number of iterations

5.4 Neural Network Training

The data collected from the experiment was then used to train a neural network consisting of 2 hidden layers with 400 and 300 neurons respectively. The sci-kit learn library in Python was used to perform this supervised learning using the data set collected. The rectified linear unit (ReLU) was used as an activation function while an adaptive learning rate was applied during the training of this network. The loss curve obtained during the training was plotted with respect to the number of iterations in Fig. 5.3. The neural network produced a R^2 value of 0.81 with the test data set.

Chapter 6

Control Algorithm

6.1 Algorithm

This section discusses how the control algorithm for the entire autonomous grasping works. The glove only controls the wrist and the finger motions so the first step is that the user has to manually bring the glove closer to the object that needs to be grasped. Second, the user initiates the glove and provides a weight category for the object through a voice command [20] or some other form of input. The glove does not have any vision sensors or any other form of input to detect the weight of the object. To overcome this the objects have been categorized into light, medium, and heavy. The initial weight values that are inputted into the neural network for these 3 categories are 3, 5, and 7 N respectively. Third, the glove estimates the shape of the object by flexing all the linkages till the fingers come in contact with the object and the IMU attached on the glove measures the orientation of the object. Finally, the weight, the radius, and the orientation of the object is passed on to the trained neural network to produce the force value required at each fingertip. The force at the fingertip is applied by the SEA through the linkage mechanism so the SEA output force must be obtained from the required fingertip force. The SEA output force F_{SEA} that must be applied to achieve the required fingertip force $F_{fingertip}$ can be calculated from equation 6.1.

Then, the algorithm determines the compression that must be achieved in each of the springs

present in the SEAs, both linear and rotary, to attain the required force with the help of equations 4.1 and 4.12. The motors then actuate the SEA using a PI controller to achieve the required compression which in turn will enable the glove to apply the appropriate force on each fingertip to grasp an object.

$$F_{SEA} = F_{fingertip}/Lev \tag{6.1}$$

where Lev is the leverage of the linkage mechanism which can be calculated based on the angle of the linkage from equations 4.7 to 4.11, F_{SEA} is the force output from the SEA shaft, and $F_{fingertip}$ is the force output at the tip of the linkage.

6.2 Force Update

To grasp an object successfully, the controller should detect changes in the environment and update the outputs accordingly. The algorithm used in the RML Glove V3 has the ability to update forces based on the changes detected during grasping. Two factors can trigger an update in the fingertip forces, namely, a change in orientation or slippage of the object being grasped.

In case a change in angular orientation of the object being grasped is detected, the algorithm will use the new angular position values obtained from the IMU as the inputs for the neural network to update the forces. Secondly, if slip is detected, the weight input of the neural network is increased which results in new updated fingertip forces. The entire flowchart of the control algorithm is shown in Fig. 6.1.

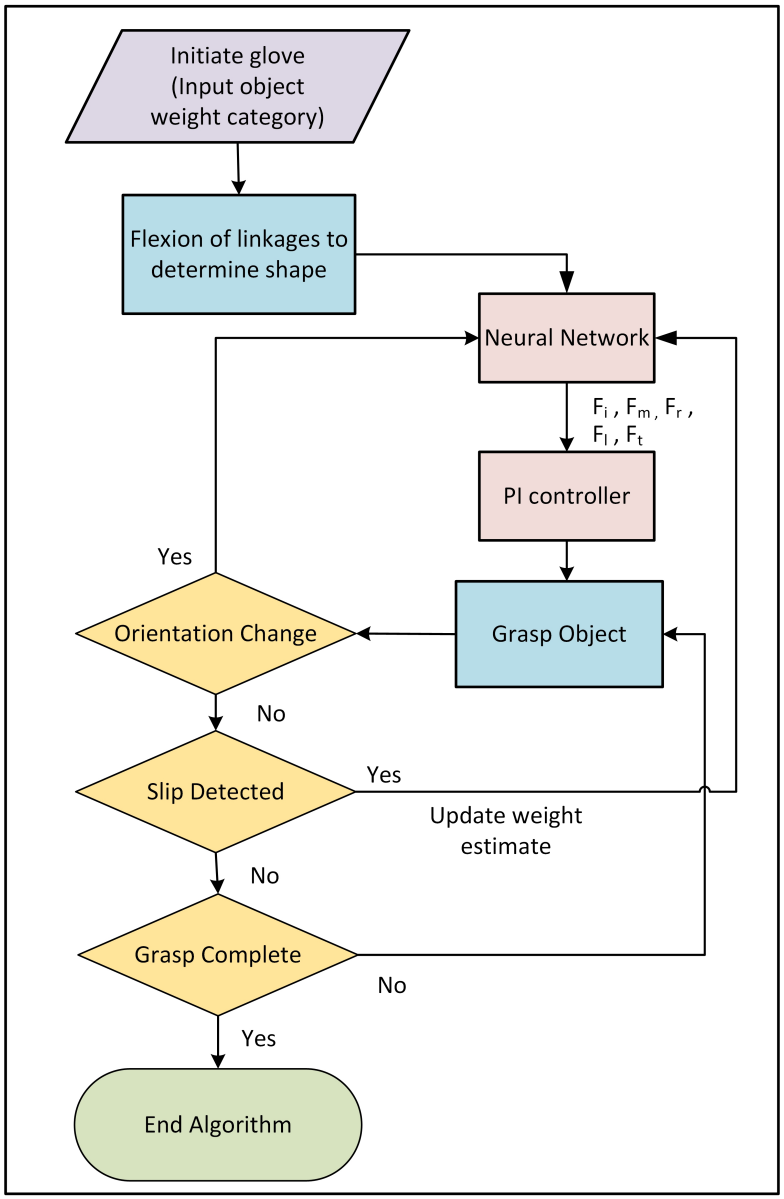

Figure 6.1: Flowchart of the semi-autonomous grasping algorithm used by the RML Glove V3

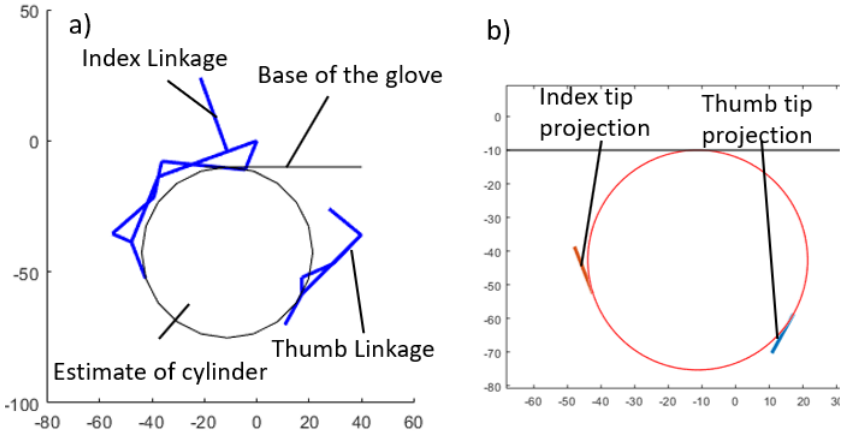

Figure 6.2: Size estimation algorithm predicting the radius of the cylindrical object being grasped from the angular positions of the index and thumb linkages

6.3 Size Estimation

The neural network requires the size of the object as one of its inputs. To determine the radius of the object, the glove has to first perform an initial grasp to just touch the object. The glove flexes all of the finger linkage mechanisms in order to come in contact with the object. This contact with the object can be detected by observing the increase in force measured through the SEAs. Then, the angular position values of all the linkages which can be measured through the potentiometer are used to determine the kinematics of the index and thumb linkages as shown in Fig. 6.2 a). The base of the glove, thumb linkage tip, and the index linkage tip are projected onto a 2D plane as shown in Fig. 6.2 b). Finally, a circle with an appropriate diameter is calculated which has these three lines as its tangents. The diameter of this circle is the size estimate of the object being grasped by our exoskeleton.

Chapter 7

Experimental Results

7.1 Unsuccessful Grasp and Correction Factor

Initially, the experiment was conducted and an attempt was made to grasp an object. The neural network estimated the fingertip forces based on the inputs which were then converted to their respective spring deflection values and passed on to the PI controller to achieve the required forces to grasp. However, the grasp was unsuccessful as shown in Fig. 7.1. This can be attributed to many factors which are stated as follows:

- Buckling and bending of the linkage mechanism which results in less force being transmitted to the fingertip.
- Frictional losses at the linkage joints and the SEA.
- Loss in surface area of contact with the object due to straps covering a part of the fingertip.
- Error in the calculation of the SEA output shaft deflection due to the inaccuracy of the angular position value obtained from the potentiometer and a low sample rate of data collection.

To account for all of these modeling errors, a correction factor of 2 was chosen by trial and error which is multiplied to each of the index, middle, ring, and little finger deflections

Figure 7.1: a) Grasp initialization, b) Unsuccessful grasp of the object

obtained after all of the calculations. The thumb mechanism does not face such problems as it does not use a double four-bar mechanism and consists of a rotary SEA. Now, the experiments were conducted using this correction factor and the results are described in the section below.

7.2 Experiment with Correction Factor

The experiment was conducted using a bottle with a radius of 85mm and a weight of 500g. The glove initially grasped the object and estimated the radius of the bottle to be 85.95mm. Then, it used the user input of the medium weight category, the angular orientation values provided by the IMU, and the estimated size, to predict the fingertip forces of 1.93, 3.20, 2.69, 1.40, and 7.02 N at the index, middle, ring, and little finger; and the thumb respectively which were then converted to the required compression values which were 2.0mm, 2.0mm, 2.0mm, 3.1mm, and 117.1 degrees respectively. The glove then successfully grasped the

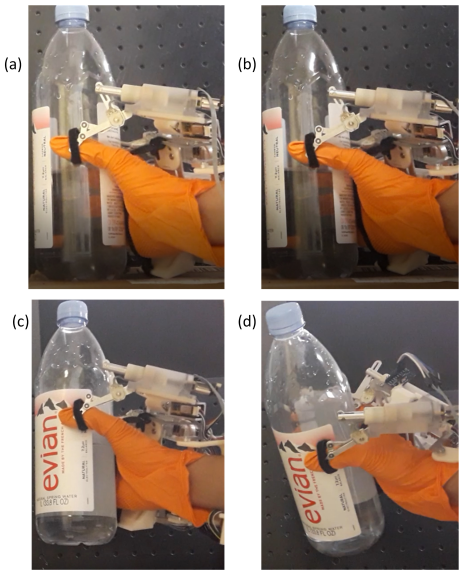

Figure 7.2: a) Grasp initialization, b) Size estimation, c) Successful grasp of a bottle with the exoskeleton glove, d) Maintaining a successful grasp even when the bottle was titled by updating the fingertip forces

object autonomously and it was lifted by the user as shown in Fig. 7.2 c).

The object being grasped was tilted from a roll and pitch value of 9.1 and -16 degrees respectively to 39.3 and -36.8 degrees at 24.5 seconds by the user. This resulted in the algorithm updating the set of inputs and generating a new set of fingertip forces through the neural network which were 2.56, 3.90, 3.45, 1.82, and 10.54 N respectively. This transforms into spring deflection values of 2.2mm, 2.5mm, 2.0mm, 4.0mm, and 120.0 degrees respectively. The user was successful in grasping the object throughout the process of rotating it as shown in Fig. 7.2 d). The fingertip forces during the experiment were measured by the SEAs and are plotted in Fig. 7.3. It can be observed from the plots that there is an increase in fingertip forces at all the digits except the thumb after the object was tilted at 24.5 second mark. The thumb force did not increase as the RSEA had already reach its limit while the rest of the linkages exerted more force due to the neural network increasing the force output.

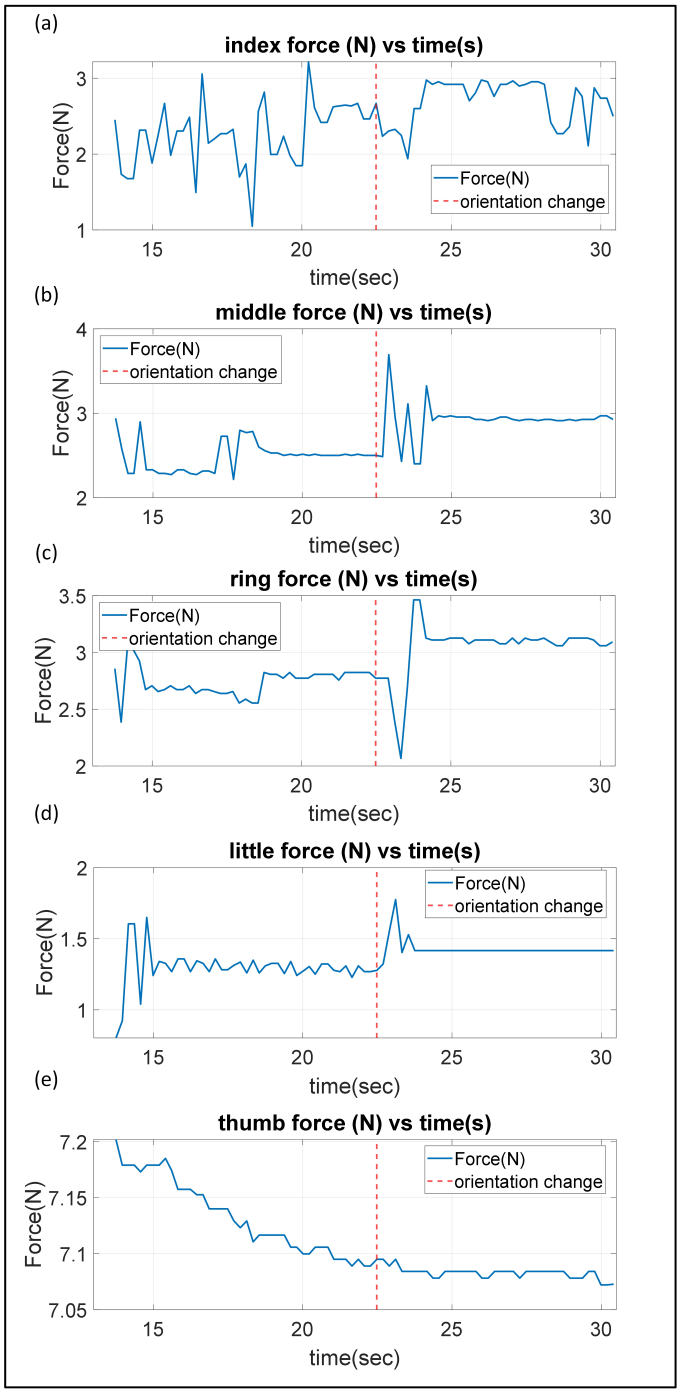

Figure 7.3: Fingertip force data recorded by the SEA during the object grasping

Chapter 8

Conclusion and Future Work

8.1 Conclusion

The thesis first discussed the design and control of the state of the art exoskeleton gloves and then our glove, the RML Glove V3, was introduced. Then, the mechanical design of the RML Glove V3 was discussed which presented a new version of the RSEA and other mechanisms which improved the comfort and adjust-ability for users of different hand sizes. Then, a neural network based control algorithm was introduced which determines the force output required in each fingertip to grasp objects at various orientations. The initial experiments were unsuccessful at grasping, so a correction factor was used which resulted in the control algorithm overcoming the modeling errors and grasping objects successfully. The exoskeleton also maintained a successful grasp when the object was tilted by updating the fingertip forces.

8.2 Future Work

This section discusses the improvements that can be made to improve the design and control of the exoskeleton glove in the future. The current neural network was trained only for cylindrical objects, but the same procedure can be applied to collect data and train the glove to grasp a variety of objects.

8.2.1 Increasing Mechanical Leverage

The design of the exoskeleton glove has some limitations like a low mechanical leverage of the linkage mechanism. This can be improved by introducing a new linkage mechanism or by changing the position of the SEAs. This will enable the glove to exert more force at the fingertips.

8.2.2 Accurate Force Sensors

The FSRs used in the experiment to collect fingertip force data from different subjects were very noisy and the accuracy of the whole algorithm can be improved by using better force sensors for data collection.

8.2.3 Accurate Potentiometers

The potentiometers used to measure the angle of the linkage mechanisms were very noisy due to which the glove was unable to detect slip. This is why the force update due to slippage of the object could not be demonstrated in an experiment. Accurate sensors for measuring angular position can eliminate this problem and enable the glove to update the fingertip forces when slip is detected.

Bibliography

[1] A. Sharma, J. S. Roo, and J. Steimle, "Grasping Microgestures," no. Chi, pp. 1–13, 2019.

[2] T. Vanteddu and P. Ben-Tzvi, "Stable Grasp Control with a Robotic Exoskeleton Glove," *Journal of Mechanisms and Robotics*, vol. 12, no. 6, pp. 1–14, 2020.

[3] M. Fontana, A. Dettori, F. Salsedo, and M. Bergamasco, "Mechanical design of a novel hand exoskeleton for accurate force displaying," *Proceedings - IEEE International Conference on Robotics and Automation*, pp. 1704–1709, 2009.

[4] B. J. Lee, A. Williams, and P. Ben-Tzvi, "Intelligent Object Grasping with Sensor Fusion for Rehabilitation and Assistive Applications," *IEEE Transactions on Neural Systems and Rehabilitation Engineering*, vol. 26, no. 8, pp. 1556–1565, 2018.

[5] J. Lee and J. Bae, "Design of a hand exoskeleton for biomechanical analysis of the stroke hand," *IEEE International Conference on Rehabilitation Robotics*, vol. 2015-Septe, pp. 484–489, 2015.

[6] D. Marconi, A. Baldoni, Z. McKinney, M. Cempini, S. Crea, and N. Vitiello, "A novel hand exoskeleton with series elastic actuation for modulated torque transfer," *Mechatronics*, vol. 61, pp. 69–82, 2019.

[7] D. Popov, I. Gaponov, and J. H. Ryu, "Portable exoskeleton glove with soft structure for hand assistance in activities of daily living," *IEEE/ASME Transactions on Mechatronics*, vol. 22, no. 2, pp. 865–875, 2017.

[8] H. In, B. B. Kang, M. K. Sin, and K. J. Cho, "Exo-Glove: A wearable robot for the hand with a soft tendon routing system," *IEEE Robotics and Automation Magazine*, vol. 22, no. 1, pp. 97–105, 2015.

[9] A. Mohammadi, J. Lavranos, P. Choong, and D. Oetomo, "Flexo-glove: A 3D Printed Soft Exoskeleton Robotic Glove for Impaired Hand Rehabilitation and Assistance," *Proceedings of the Annual International Conference of the IEEE Engineering in Medicine and Biology Society, EMBS*, vol. 2018-July, pp. 2120–2123, 2018.

[10] C. G. Rose and M. K. O'Malley, "Hybrid Rigid-Soft Hand Exoskeleton to Assist Functional Dexterity," *IEEE Robotics and Automation Letters*, vol. 4, no. 1, pp. 73–80, 2019.

[11] L. Gerez, G. Gao, A. Dwivedi, and M. Liarokapis, "A Hybrid, Wearable Exoskeleton Glove Equipped With Variable Stiffness Joints, Abduction Capabilities, and a Telescopic Thumb," *IEEE Access*, vol. 8, pp. 173345–173358, 2020.

[12] F. Ficuciello, A. Migliozzi, G. Laudante, P. Falco, and B. Siciliano, "Vision-based grasp learning of an anthropomorphic hand-arm system in a synergy-based control framework," *Science Robotics*, vol. 4, no. 26, 2019.

[13] National Spinal Cord Injury Statistical Center, "Spinal cord injury facts and figures at a glance.," *The journal of spinal cord medicine*, vol. 36, no. 1, pp. 1–2, 2013.

[14] D. Mozaffarian, E. J. Benjamin, A. S. Go, D. K. Arnett, M. J. Blaha, M. Cushman, S. R. Das, S. D. Ferranti, J. P. Després, H. J. Fullerton, V. J. Howard, M. D. Huffman, C. R. Isasi, M. C. Jiménez, S. E. Judd, B. M. Kissela, J. H. Lichtman, L. D. Lisabeth, S. Liu, R. H. MacKey, D. J. Magid, D. K. McGuire, E. R. Mohler, C. S. Moy, P. Muntner, M. E. Mussolino, K. Nasir, R. W. Neumar, G. Nichol, L. Palaniappan, D. K. Pandey,

M. J. Reeves, C. J. Rodriguez, W. Rosamond, P. D. Sorlie, J. Stein, A. Towfighi, T. N. Turan, S. S. Virani, D. Woo, R. W. Yeh, and M. B. Turner, *Heart disease and stroke statistics-2016 update a report from the American Heart Association*, vol. 133. 2016.

[15] E. Refour, B. Sebastian, and P. Ben-Tzvi, "Two-digit robotic exoskeleton glove mechanism: Design and integration," *Journal of Mechanisms and Robotics*, vol. 10, no. 2, pp. 1–9, 2018.

[16] E. M. Refour, B. Sebastian, R. J. Chauhan, and P. Ben-Tzvi, "A General Purpose Robotic Hand Exoskeleton With Series Elastic Actuation," *Journal of Mechanisms and Robotics*, vol. 11, 09 2019. 060902.

[17] *Sensing and Force-Feedback Exoskeleton Robotic (SAFER) Glove Mechanism for Hand Rehabilitation*, vol. Volume 5A: 39th Mechanisms and Robotics Conference of *International Design Engineering Technical Conferences and Computers and Information in Engineering Conference*, 08 2015. V05AT08A036.

[18] W. Xu, S. Pradhan, Y. Guo, C. Bravo, and P. Ben-Tzvi, "A Novel Design of a Robotic Glove System for Patients With Brachial Plexus Injuries," vol. Volume 10: 44th Mechanisms and Robotics Conference (MR) of *International Design Engineering Technical Conferences and Computers and Information in Engineering Conference*, 08 2020. V010T10A042.

[19] T. Vanteddu, B. Sebastian, and P. Ben-Tzvi, "Design optimization of RML glove for improved grasp performance," *ASME 2018 Dynamic Systems and Control Conference, DSCC 2018*, vol. 1, pp. 1–8, 2018.

[20] Y. Guo, W. Xu, S. Pradhan, C. Bravo, and P. Ben-Tzvi, "Integrated and Configurable Voice Activation and Speaker Verification System for a Robotic Exoskeleton Glove,"

vol. Volume 10: 44th Mechanisms and Robotics Conference (MR) of *International Design Engineering Technical Conferences and Computers and Information in Engineering Conference*, 08 2020. V010T10A043.